CrystEngComm

Accepted Manuscript

ROYAL SOCIETY OF CHEMISTRY

www.rsc.org/crystengcomm

Cite this: DOI: 10.1039/c0xx00000x

www.rsc.org/xxxxxx

ARTICLE TYPE

fiAdamantane Derivatives of Sulfonamide Molecular Crystals: Structure, Sublimation Thermodynamic Characteristics, Molecular Packing, Hydrogen Bonds Networks

German L. Perlovich*[a,b], Alex M. Ryzhakov[a,b], Valery V. Tkachev[b,c] and Alexey N. Proshin[b]

Received (in XXX, XXX) Xth XXXXXXXXX 200X, Accepted Xth XXXXXXXXX 200X
DOI: 10.1039/b000000x

The crystal structures of six adamantane derivatives of sulfonamides have been determined by X-ray diffraction. The molecular conformational states, packing architecture, and hydrogen bond networks were analyzed. Conformational flexibility of the bridge connecting the phenyl ring and the adamantine fragment was studied. The molecular packing architectures of the selected crystals can be for convenience divided into three different groups. The thermodynamic aspects of sublimation processes of the compounds were studied by determining the temperature dependence of vapor pressure using the transpiration method. The thermophysical characteristics of fusion processes of the molecular crystals were obtained and analyzed. Correlations between the sublimation thermodynamic functions and physico-chemical descriptors were revealed. A regression equation connecting the sublimation Gibbs energies and van der Waals's molecular volumes was derived. The influence of various molecular fragments on crystal lattice energy was analyzed. A relationship between the melting points of the studied substances and the free volumes per molecule in the crystal lattices was evaluated.

Introduction

Sulfonamides (SA) are an important class of therapeutic agents in modern medical science.[1] Sulfonamides are capable of many types of biological activity such as antibacterial,[2] hypoglycemic,[3] diuretic,[4] and antiglaucoma[5,6] action. Recently, many structurally novel aryl sulfonamides have been reported to have significant antitumor activity.[7-9,11] Atrial fibrillation (AF) is the most common cardiac arrhythmia, and patients suffering from AF generally have a reduced quality of life with a lower cardiac output and impaired ability to work and exercise. AF patients also have an increased risk of stroke and other cardiovascular diseases. Olsson et al.[10] described and evaluated a novel class of lactam sulfonamides in order to find a potent selective inhibitor for regulation of the potassium ion channel responsible for AF.

No other singular hydrocarbon moiety (apart from the methyl group) is as successful as adamantane in improving or providing pharmacological activity in and of bestselling pharmaceuticals. Having the "lipophilic bullet" (adamantane is often viewed as providing only the critical lipophilicity) readily available as an "add-on" for known pharmacophors, adamantane was used in the modification of, for example, hypoglycemic sulfonylureas[12], anabolic steroids[13], and nucleosides.[14] The adamantane modifications were chosen to enhance lipophilicity and stability of the drugs, thereby improving their pharmacokinetics. Aminoadamantanes, such as amantadine[15], rimantadine[16] and tromantadine[17] were among the first "hits" that successfully made it to the pharmaceutical market, and most of them are still in use. These remarkable bottom-of-the-line structures are not only efficiently used as pharmaceuticals but have also improved the understanding of the molecular mechanisms underlying, for example, the replication of Influenza A viruses. Adamantane derivatives have been used as antimalarials.[18,19] Frequently, the addition of adamantane moieties increases the permeability of the modified compound through the blood−brain barrier.[20] Therefore, targets of the central nervous system (CNS) today are probably most promising both academically and commercially. With the fortuitous finding that amantadine gives symptomatic benefits in Parkinson disease[21] and the approval of memantine by EMA and FDA for the treatment of moderate to severe stages of Alzheimer disease,[22] two neurodegenerative diseases of increasing importance in aging societies are being addressed with (structurally again remarkably simple) adamantane derivatives.

Since many sulfonamides are poorly soluble in aqueous solutions, structural modification of the molecule by adding an adamantane fragment can lead to both membrane permeability increase and aqueous solubility improvement. This effect may be caused by a decrease in the crystal lattice Gibbs energy of the compounds owing to "friable" (with a free volume excess) molecular packing in the crystals.

Sulfonamides with different adamantane fragments were selected as the objects of the investigations (Fig. 1). This class of substances is quite promising due to their application as neuroprotectors in Alzheimer disease correction. The paper opens a cycle of works devoted to the comprehensive study of the outlined compounds in solid state (crystal structure, sublimation and fusion processes) and in solutions (solubility, solvation, distribution and transfer processes in different biological mediums).

Cite this: DOI: 10.1039/c0xx00000x

www.rsc.org/xxxxxx

ARTICLE TYPE

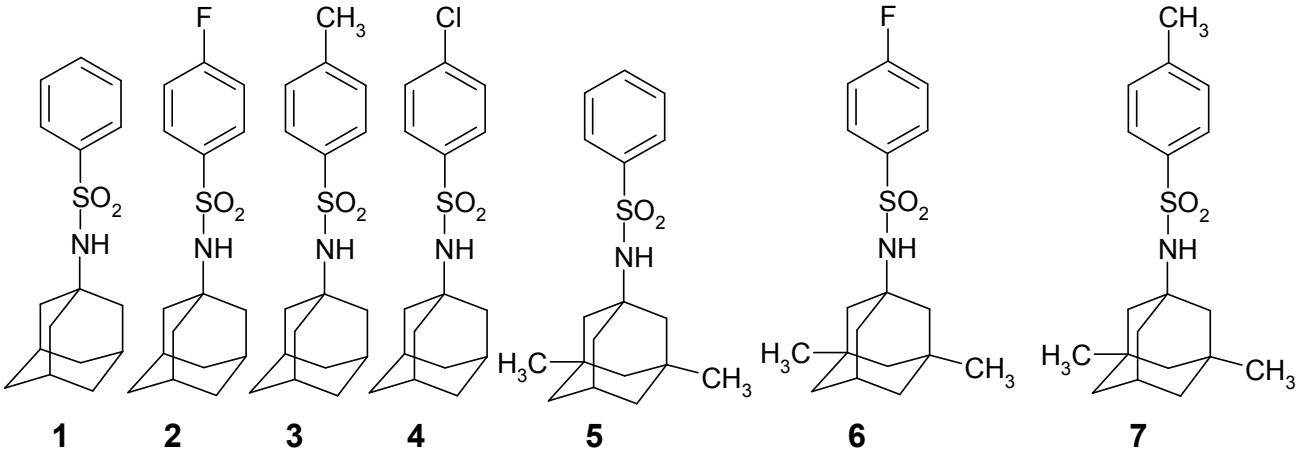

Fig. 1 Structural formulas of the compounds studied

Experimental

Synthesis

General procedure of the synthesis of the compounds studied

Synthesis of the novel sulfonamide derivatives was carried out according to Scheme 1.

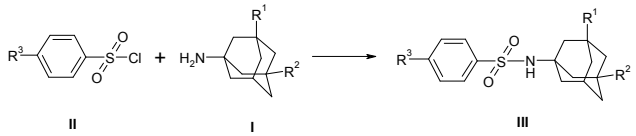

Scheme 1

Triethylamine (0.04 mol) was added to a stirred suspension of 1-aminoadamantane **I** (or Memantine, R^1, R^2 = CH_3) (0.01 mol) in isopropanol (30 ml) at 0°C, followed by solid sulfonyl chloride **II** (R^3 = H, CH_3, Cl, F) (0.01 mol) over a period of 30 minutes. The reaction mixture was heated at 60°C for 2 hours, after which HPLC showed that there was no starting material left. The resulting suspension was cooled to room temperature and the precipitate of triethylamine hydrochloride was removed by filtration. The filtrate was evaporated to dryness to afford a colourless oil which was dissolved in ethyl acetate (50 ml), washed with 0.5N HC1 (50 ml), water (50 m1) and dried over $MgSO_4$. The solvent was evaporated by a rotary evaporator to afford sulfonamide as a white crystalline solid. Yields: 80-90%.

The compounds were carefully purified by re-crystallizing from water-ethanol solution. The precipitate was filtered and dried at room temperature under vacuum until the mass of compounds remained constant. The outlined procedure was repeated several times and the product checked by NMR after each re-crystallization step until the proton NMR signal correspondence to the purity of the compound was over 99 %.

NMR Experiments

^{1}H NMR spectra were recorded on Bruker CXP-200 instrument (Germany). As a solvent it was applied $CDCl_3$.

N-Adamantan-1-yl-benzenesulfonamide (**1**)
^{1}H NMR (200 MHz, $CDCl_3$), δ, ppm: 1.28 - 1.62 (m, 6H, AdH), 1.679 (d, *J* = 2.79 Hz, 6H, AdH), 1.91 (br. s., 3H, AdH), 4.58 (s, 1H, NH), 7.37 - 7.60 (m, 3H, ArH), 7.89 (dd, *J* = 7.58, 1.20 Hz, 2H, ArH). Mp 124.3 ± 0.2 °C. Anal. ($C_{16}H_{21}NO_2S$) C, H, N, S.

N-Adamantan-1-yl-4-fluoro-benzenesulfonamide (**2**)
^{1}H NMR (200 MHz, $CDCl_3$), δ, ppm: 1.47 - 1.77 (m, 6H, AdH), 1.77 - 1.93 (m, 6H, AdH), 2.05 (br. s., 3H, AdH), 4.64 (br. s., 1H, NH), 7.20 (t, *J* = 8.84 Hz, 2H, ArH), 7.83 - 8.09 (m, 2H, ArH). Mp 146.2 ± 0.2 °C. Anal. ($C_{16}H_{20}FNO_2S$) C, H, N, S.

N-Adamantan-1-yl-4-methyl-benzenesulfonamide (**3**)
^{1}H NMR (200 MHz, $CDCl_3$), δ, ppm: 1.30 - 1.62 (m, 6H, AdH), 1.70 (d, *J* = 2.79 Hz, 6H, AdH), 1.95 (br. s., 3H, AdH), 2.44 (s, 3H, CH_3), 4.62 (s, 1H, NH), 7.16 - 7.35 (d, *J* = 7.83 Hz, 2H, ArH), 7.78 (d, *J* = 7.83 Hz, 2H, ArH). Mp 164.7 ± 0.2 °C. Anal. ($C_{17}H_{23}NO_2S$) C, H, N, S.

N-Adamantan-1-yl-4-chloro-benzenesulfonamide (**4**)
^{1}H NMR (200 MHz, $CDCl_3$), δ, ppm: 1.30 - 1.62 (m, 6H, AdH), 1.69 (d, *J* = 2.79 Hz, 6H, AdH), 1.93 (br. s., 3H, AdH), 4.60 (s, 1H, NH), 7.28 - 7.49 (m, 2H, ArH), 7.67 - 7.86 (m, 2H, ArH). Mp 186.8 ± 0.2 °C. Anal. ($C_{16}H_{20}ClNO_2S$) C, H, N, S.

N-(3,5-Dimethyl-adamantan-1-yl)-benzenesulfonamide (**5**)
^{1}H NMR (200 MHz, $CDCl_3$), δ, ppm: 0.77 (s, 6H, $2CH_3$), 1.06 (s, 2H, AdH), 1.10 - 1.31 (m, 4H, AdH), 1.31 - 1.55 (m, 4H, AdH), 1.55 - 1.71 (m, 2H, AdH), 1.92 - 2.15 (m, 1H, AdH), 4.86 (br. s., 1H, NH), 7.37 - 7.60 (m, 3H, ArH), 7.91 (dd, *J* = 7.58, 1.22 Hz, 2H, ArH). Mp 143.2 ± 0.2 °C. Anal. ($C_{18}H_{25}NO_2S$) C, H, N, S.

N-(3,5-Dimethyl-adamantan-1-yl)-4-fluoro-benzenesulfonamide (**6**)
^{1}H NMR (200 MHz, $CDCl_3$), δ, ppm:0.73 (s, 6H, $2CH_3$), 1.02 (s, 2H, AdH), 1.10 - 1.29 (m, 4H, AdH), 1.31 - 1.53 (m, 4H, AdH), 1.53 - 1.70 (m, 2H, AdH), 1.90 - 2.12 (m, 1H, AdH), 4.70 (br. s., 1H, NH), 6.95 - 7.22 (m, 2H, ArH), 7.78 - 8.03 (m, 2H, ArH).

Mp 137.3 ± 0.2 °C. Anal. ($C_{18}H_{24}FNO_2S$) C, H, N, S.

N-(3,5-Dimethyl-adamantan-1-yl)-4-methyl-benzenesulfonamide (**7**)

^{1}H NMR (200 MHz, $CDCl_3$), δ, ppm: 0.77 (s, 6H, $2CH_3$), 1.06 (s, 2H, AdH), 1.12 - 1.32 (m, 4H, AdH), 1.32 - 1.55 (m, 4H, AdH), 1.55 - 1.67 (m, 2H, AdH), 1.98 - 2.11 (m, 1H, AdH), 2.42 (s, 3H, $ArCH_3$), 4.68 (br. s., 1H, NH), 7.16 - 7.35 (d, J = 7.83 Hz, 2H, ArH), 7.78 (d, J = 7.83 Hz, 2H, ArH). Mp 162.4 ± 0.2 °C. Anal. ($C_{19}H_{27}NO_2S$) C, H, N, S.

Single crystals preparation

Single crystals of compounds **1** and **3** were grown from an ethanol solution by slow evaporation. Single crystals of substances **4**, **5** and **6** were prepared from an isopropyl solution (the initial composition 20:1 v/v) by slow evaporation. Finally, single crystals of **7** were yielded from an (isopropyl ethanol – ethyl acetate) solution by slow evaporation.

Methods

X-ray diffraction experiments. Single-crystal X-ray measurements were carried out using a Nonius CAD-4 diffractometer with graphite-monochromated Mo K_α radiation (λ = 0.71069 Å). The intensity data were collected at 25° C by means of a ω-2θ scanning procedure. The crystal structures were solved using direct methods and refined by means of a full-matrix least-squares procedure. CAD-4[23] was applied for data collection, data reduction and cell refinement. The SHELXS-97 and SHELXL-97 programs[24] were used to solve and to refine structures, respectively.

Sublimation experiments. Sublimation experiments were carried out by the transpiration method as was described elsewhere.[25] In brief: a stream of an inert gas passes above the sample at a constant temperature and at a known slow constant flow rate in order to achieve saturation of the carrier gas with the vapor of the substance under investigation. The vapor is condensed at some point downstream, and the mass of sublimate and its purity are determined. The vapor pressure over the sample at this temperature can be calculated by the amount of the sublimated sample and the volume of the inert gas used.

The equipment was calibrated using benzoic acid. The standard value of sublimation enthalpy obtained here was ΔH^0_{sub} = 90.5 ± 0.3 J·mol^{-1}. This is in good agreement with the value recommended by IUPAC of ΔH^0_{sub} = 89.7 ± 0.5 J·mol^{-1}.[26] The saturated vapor pressures were measured 5 times at each temperature with the standard deviation being within 3-5 %. Because the saturated vapor pressure of the investigated compounds is low, it can be assumed that the change of the vapor heat capacity with the temperature is so small that it can be neglected. The experimentally determined vapor pressure data may be described in (lnP;1/T) co-ordinates in the following way:

$$\ln(P) = A + B/T \qquad (1)$$

The value of the sublimation enthalpy is calculated by the Clausius-Clapeyron equation:

$$\Delta H^T_{sub} = RT^2 \cdot \partial(\ln P)/\partial(T) \qquad (2)$$

whereas the sublimation entropy at the given temperature T is calculated from the following relation:

$$\Delta S^T_{sub} = (\Delta H^T_{sub} - \Delta G^T_{sub})/T \qquad (3)$$

with $\Delta G^T_{sub} = -RT\ln(P/P_0)$, where P_0 is the standard pressure of $1\cdot10^5$ Pa

For experimental reasons, the sublimation data are obtained at elevated temperatures. However, in comparison with effusion methods, the temperatures are much lower, which makes extrapolation to room conditions easier. In order to further improve the extrapolation to room conditions, we estimated the heat capacities ($C^{298}_{p,cr}$-value) of the crystals using the additive scheme proposed by Chickos et al.[27] Heat capacity was introduced as a correction for the recalculation of the sublimation enthalpy ΔH^T_{sub}-value at 298 K (ΔH^{298}_{sub}-value), according to the equation[27]:

$$\Delta H^{298}_{sub} = \Delta H^T_{sub} + \Delta H_{cor} =$$

$$= \Delta H^T_{sub} + (0.75 + 0.15\cdot C^{298}_{p,cr})\cdot(\text{T-298.15}) \qquad (4)$$

Differential scanning calorimetry. Differential scanning calorimetry (DSC*)* was carried out using a Perkin-Elmer Pyris 1 DSC differential scanning calorimeter (Perkin Elmer Analytical Instruments, Norwalk, Connecticut, USA) with Pyris software for Windows NT. DSC runs were performed in an atmosphere of flowing (20 ml·min^{-1}) dry helium gas of high purity 99.996% using standard aluminum sample pans and at a heating rate of 10 K·min^{-1}. The accuracy of weight measurements was ± 0.005 mg. The DSC was calibrated with an indium sample from Perkin-Elmer (P/N 0319-0033). The value determined for the enthalpy of fusion corresponded to 28.48 J·g^{-1} (reference value 28.45 J·g^{-1}). The melting point was 156.5±0.1° C (n=10).

Calculation procedure. The free molecular volume in the crystal lattice was estimated on the basis of the X-ray diffraction data and van der Waals molecular volume (V^{vdw}), calculated by GEPOL[28]:

$$V^{free} = (V_{cell} - Z\cdot V^{vdw})/Z \qquad (5)$$

where V_{cell} is the volume of the unit cell, Z is the number of molecules in the unit cell.

Non-bonded van der Waals interactions of crystal lattice energy were calculated as a sum of atom-atom interactions with the help of Gavezzotti et al.[29] force field and cut-off radius 16 Å.

Physicochemical descriptors applied in the analysis of solubility and transfer processes were estimated by means of the program HYBOT (**HY**drogen **BO**nd **T**hermodynamics).[30]

Results and Discussion

Crystal Structure Analysis

The results of X-ray diffraction experiments are presented in Table 1. The numbering of atoms of the considered compounds was unified and exemplified by compound **4** (Fig. 2). Hydrogen bond geometry and graph set notations of the molecules studied

are summarized in Table 2

Table 1 Crystal lattice parameters of the substances under investigation[a]

	1	**3**	**4**	**5**	**6**	**7**
CCDC code	1028779	1028778	1028780	1028783	1028782	1028781
crystal system	orthorhombic	monoclinic	monoclinic	monoclinic	monoclinic	monoclinic
space group	$Pca2_1$	$P2_1/c$	$P2_1/c$	$P2_1/n$	$P2_1/n$	$P2_1/n$
crystal size, mm	0.38×0.34×0.22	0.31×0.26×0.20	0.40×0.35×0.15	0.40×0.37×0.30	0.45×0.40×0.35	0.43×0.27×0.15
a, Å	11.977(1)	11.189(2)	11.0510(4)	9.3350(2)	10.5261(1)	10.8028(3)
b, Å	10.516(1)	6.536(1)	6.4458(3)	11.5770(2)	11.5499(1)	11.6083(3)
c, Å	11.290(1)	21.527(4)	21.4660(8)	15.7703(3)	14.1017(4)	14.0725(4)
α, °	90.00	90.00	90.00	90.00	90.00	90.00
β, °	90.00	102.41(3)	102.427(3)	100.587(2)	97.386(2)	95.824(3)
γ, °	90.00	90.00	90.00	90.00	90.00	90.00
volume, Å^3	1422.0(2)	1537.5(5)	1493.2(1)	1675.31(6)	1700.20(8)	1755.61(8)
Z	4	4	4	4	4	4
D_{calc}, g·cm^{-3}	1.361	1.319	1.449	1.267	1.318	1.262
radiation	Mo K_α	Mo K_α	Mo K_α	Mo K_α	Mo K_α	Mo K_α
T, K	293(2)	293(2)	150.0(1)	150(1)	150(1)	100(1)
μ, мм$^{-1}$	0.229	0.215	0.399	0.20	0.209	0.19
Data collection						
measured reflections	1789	3097	7450	8683	8870	9233
independed reflections	1458	3010	3990	4475	4527	4679
independed reflections with > 2σ(I)	1365	2331	3442	3753	3840	4098
R_{int}	0.029	0.010	0.016	0.018	0.015	0.021
θ_{max}, °	25.0	26.0	29.1	29.1	29.1	29.1
Refinement						
refinement on	F^2	F^2	F^2	F^2	F	F^2
$R[F^2>2\sigma(F^2)]$	0.0299	0.0468	0.0361	0.0381	0.0356	0.0355
$\omega R(F^2)$	0.0733	0.1609	0.0924	0.1038	0.0925	0.0989
S	1.067	1.030	1.067	1.046	1.045	1.021
reflections	1458	3010	3990	4475	4527	4679
parameters	185	192	190	196	208	211
$(\Delta/\sigma)_{max}$	<0.001	<0.001	<0.001	0.001	<0.010	<0.001
$\Delta\rho_{max}$, e· Å^{-3}	0.197	0.626	0.363	0.341	0.300	0.381
$\Delta\rho_{min}$, e· Å^{-3}	-0.131	-0.434	-0.424	-0.421	-0.364	-0.431
V^{vdw}, Å^3	246.3	263.6	265.1	280.2	282.8	295.7
V^{free}, Å^3	109.2	120.8	108.2	138.6	142.2	143.2
$\beta = V^{free}/V^{vdw}$, %	44.3	45.8	40.8	49.5	50.3	48.4
$K = V^{vdw}/V_{mol}$, %	69.3	68.6	71.0	66.9	66.5	67.4

[a] Standard deviations are presented in brackets;

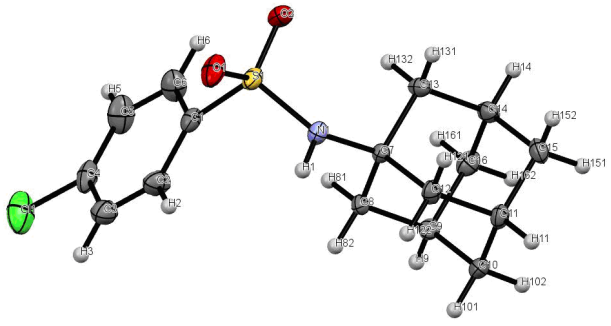

Fig. 2 Unified numbering of atoms of the considered compounds (exemplified by compound **4)**

The hydrogen bonds of the selected crystals create hydrogen bond networks with various topological structures. To analyze hydrogen bond networks topology, we used graph set notation terminology introduced by Etter[31] and supplemented by Bernstein[32]. The comparative characteristics of the hydrogen bonds geometry and matrix of the topological graphs describing hydrogen bond networks topology of the molecular crystals are presented in Table 2. The topological graphs occurring in the studied crystals are shown in Scheme 2. Two compounds (**3** and **4**) create hydrogen bond networks including infinite chains with four included atoms C(4), whereas three substances (**5**, **6** and **7**) generate dimers with set graph notation $R_2^2(8)$.

Cite this: DOI: 10.1039/c0xx00000x

www.rsc.org/xxxxxx

ARTICLE TYPE

Table 2 Hydrogen bonds geometry and graph set notations of the molecules studied

	D—H…A[a]	D—H	H…A	D…A	D—H…A	Graph set notation
3	N1-H1…O1^{i}	0.860	2.373	3.000	130.1	C(4)
4	N1-H1…O1^{i}	0.891	2.073	2.949	167.7	C(4)
5	N1-H1…O1^{i}	0.932	1.992	2.918	172.4	$R_2^2(8)$
6	N1-H1…O1^{i}	0.848	2.048	2.891	172.3	$R_2^2(8)$
7	N1-H1…O1^{i}	0.836	2.070	2.900	172.0	$R_2^2(8)$

[a] symmetry code: (i) x,y,z.

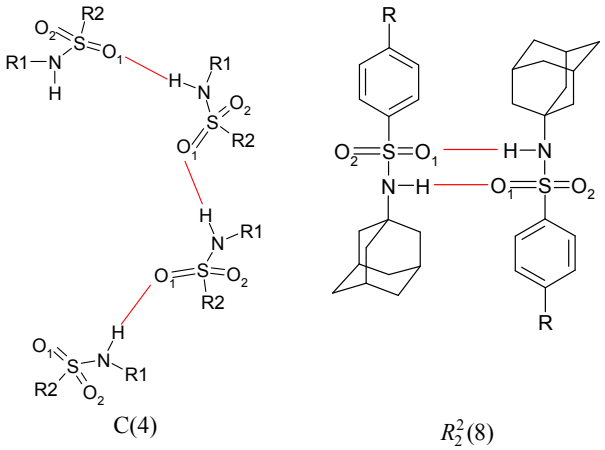

Scheme 2

Molecular conformational analysis

The conformational states of the molecules under investigation depend on the mobility of the bridge, connecting phenyl rings and adamantane fragment. Three parameters (as those used by Perlovich et al.[33]) have been chosen to describe the conformational state: the angle between the SO_2-group and the phenyl motif Ph (C1-C2-C3-C4-C5-C6) ∠C2-C1-S1-N1 (τ_1) and the angle ∠C1-N1-S1-C7 (τ_2), describing the S1-N1 bond mobility (Fig. 2). In addition to the noted angles, we introduced an angle equal to the sum of the dihedral angles ($\sum\tau_i = \tau_1+\tau_2$), which describes the integral flexibility of the bridge connecting the phenyl ring with the adamantane motif. Moreover, we introduced an angle between the phenyl ring and adamantane fragment ∠Ph-Ad (the acute angle between the least-square planes through the phenyl ring C1-C2-C3-C4-C5-C6 and the plane including atoms C7-C13-C14-C10). Experimental values of the angles are summarized in Table 3.

As it follows from Table 3, the molecules of compounds **3** and **4** have very similar conformational states. Moreover, the conformational states of **5**, **6** and **7** are similar as well.

The experimental values τ_1 (a), $\tau_1 + \tau_2$ (b) and ∠Ph-Ad (c) versus the free volume per molecule in the crystals (V^{free}) are presented in Fig. 3 (a,b,c). It should be noted that compound **1** falls out of the obtained regularities. This observation may be connected to the fact that no hydrogen bond networks are created in crystal **1** in contrast to the other compounds, where SO_2- and NH- groups participate in building of these bonds. It is evident that an increase in the free volume per molecule in the crystals reduces τ_1, ($\tau_1 + \tau_2$) and ∠Ph-Ad which tend to reach the values corresponding to the unstrained state. Thus, the flexibility of the bridge connecting the phenyl ring with the adamantane motif is very sensitive both to the free volume and to the availability of the hydrogen bonds in which the bridge takes part.

Table 3 Some parameters (°) describing molecular conformational states in the crystals studied

Compound	τ_1	τ_2	$\tau_1 + \tau_2$	∠Ph-Ad
1	28.2	83.0	111.2	99.3
3	58.2	76.4	134.6	105.4
4	58.8	76.3	135.1	105.4
5	53.8	75.1	128.9	95.7
6	47.6	78.7	126.3	94.7
7	46.4	74.5	120.9	91.4

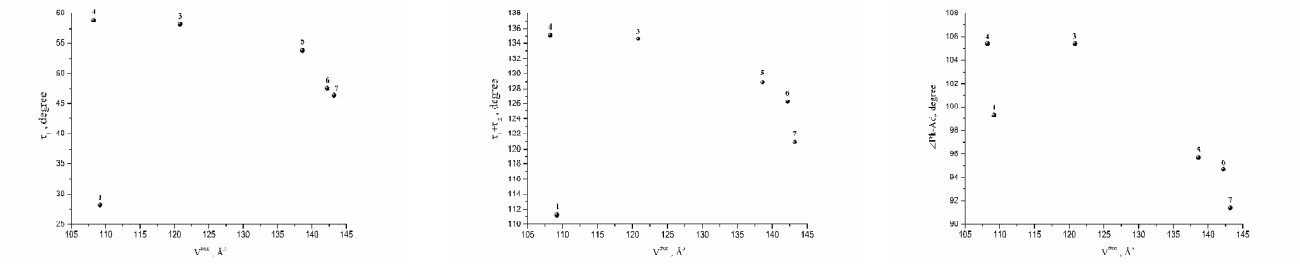

a b c

Fig. 3 The experimental values τ_1 (a), $\tau_1 + \tau_2$ (b) and ∠Ph-Ad (c) versus the free volume per molecule (V^{free}) in the crystal lattices studied

Cite this: DOI: 10.1039/c0xx00000x

www.rsc.org/xxxxxx

ARTICLE TYPE

It should be mentioned that if compounds with the same adamantane fragment (**5**, **6** and **7**) are taken into consideration, the following peculiarities of their conformational states are observed (Fig. 4). Substances **6** and **7** (Fig. 4 b, c) have a similar location of the methyl groups at the adamantane motif in relation to the axis imaginably drawn through the (N1-C7) bond and perpendicularly oriented to the plane of the Fig.4. In contract, the adamantane motif of substance **5** is rotated 120° clockwise in comparison with **6** and **7** (Fig. 4 a).

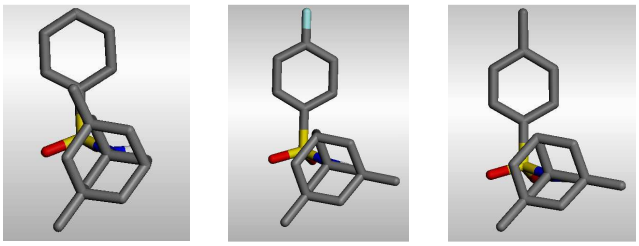

a b c

Fig. 4 Conformational states of the molecules **5** (a), **6** (b) and **7** (c) in the crystal lattices studied (H-atoms are omitted)

Packing architecture analysis

As it was noted above, the compounds studied can be for convenience divided into three groups: compounds without hydrogen bonds (**1**), those forming infinite chains C(4) (**3**, **4**) and crystals with dimer structure organization $R_2^2(8)$ (**5**, **6**, **7**).

Molecular packing architecture of crystal **1** can be presented as a zigzag layers packing (Fig. 5). Inside a layer the molecules are generally packed due to interactions between the adamantane motifs, which create the "core" of the zigzag. The sulfonamide phenyl fragments "decorate" the adamantane "core" alternately sticking out on different sides from the "core". Molecules within the layer interact with each other by van der Waals's forces. In turn, the layers interact with each other by van der Waals's forces as well. The sulfonamide phenyl fragments of each layer fill the cave of the adjacent layer topologically making the crystal lattice packing ultimately compact.

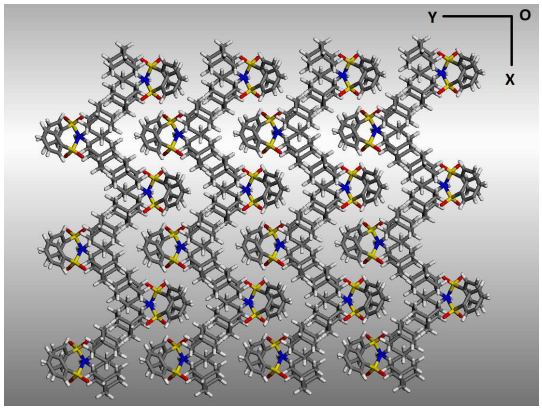

Fig. 5 Molecular packing architecture of crystal **1**

Molecular packing **3** can be presented in the following way. The hydrogen bonds, appearing between the sulfonamide bridges, form helicoids which are parallel to (OY)-axis. The centers of the helicoids are located in 1/4 and 3/4 of the distance (OZ). In turn, the mentioned chains interact with each other in the crystal by van der Waals's forces (Fig. 6 a). The molecular packing architecture of compound **4** is very similar to the previous case (Fig. 6 b).

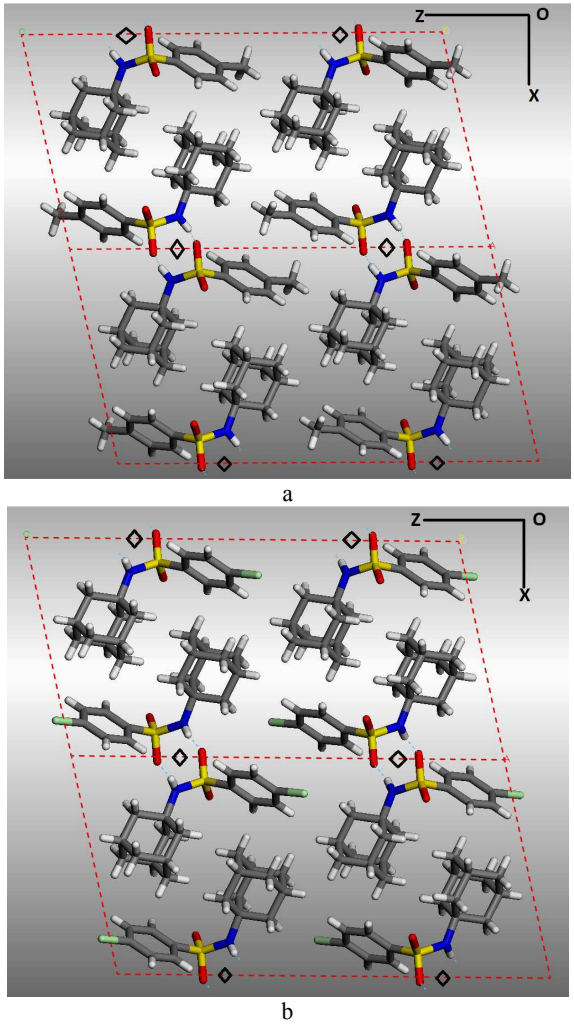

a b

Fig. 6 Molecular packing architectures of crystals **3** (a) and **4** (b). Rhombs correspond to the centers of the helicoids

Finally, the third group of the compounds (**5**, **6**, **7**) includes crystals with dimer molecular organization. Various projections of the dimers under investigation are shown in Fig. 1ESI. As it was noted above, adamantane motif **5** is rotated clockwise in relation to the (N1-C7) bond, in comparison with **6** and **7**. This fact affects the geometric structure of the dimers (the orientation of the phenyl groups in relation to the plane where the hydrogen bonds with graph set notation $R_2^2(8)$ are located). The described

effects, in their turn, influence the molecular packing architecture of the crystals. Fig. 7 and 8 show different projections of the molecular packing of compounds **6** and **7**, respectively. The molecular packing architectures of substances **6** and **7** are very similar.

The dimers of molecules **6** are uniformly packed in the plane (YOZ), i.e. it is not possible to distinguish any anisotropy within the plane). However, in a projection parallel to (XOZ), one can observe alternately interlacing layers, composed of phenyl and adamantane molecular fragments (Fig. 7 b). The adamantane motifs extend from the sulfonamide phenyl fragments of the selected dimer into the adjacent layers (above and below the imaginary plane formed by the phenyl parts of the molecules).

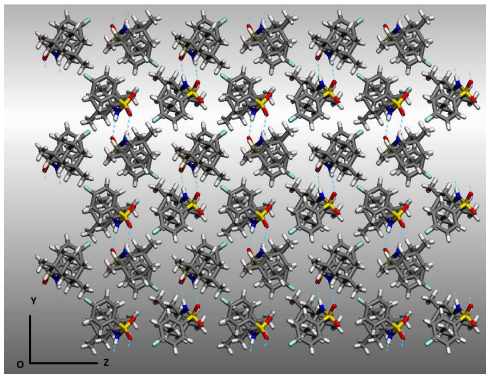

a

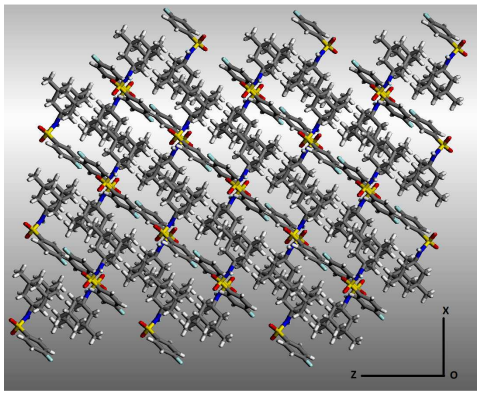

b

Fig. 7 Projections of molecular packing of crystal **6** on the planes (YOZ) – a and (XOZ) – b.

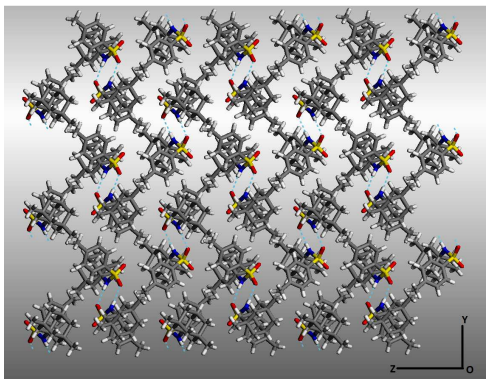

a

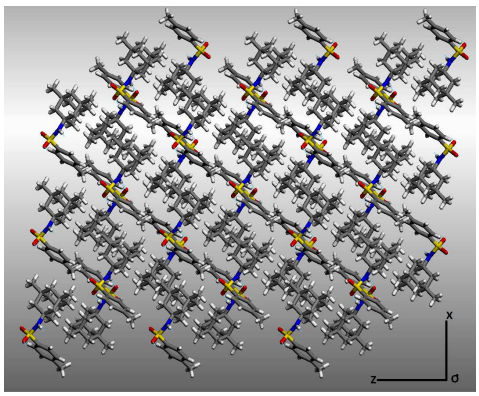

b

Fig. 8 Projections of molecular packing of crystal **7** on the planes (YOZ) – a and (XOZ) – b.

In its turn, the "adamantane" layer is composed in such a way that each adamantane motif alternately extends from the layers located above and below. This packing looks like interlaced fingers. It is this molecular packing that allows us to conclude that crystal growth from dimer saturated solution is carried out by means of delicate adjustment of the adamantane fragments into the corresponding layers. Similar conclusions can be made for compound **7** (Fig. 8 a, b).

Molecular packing architecture of compound **5** is similar to that of the two previous compounds (Fig. 9 a, b).

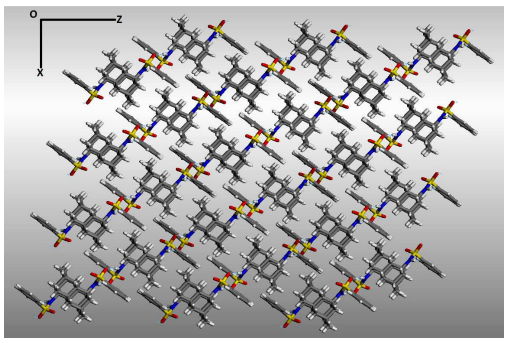

a

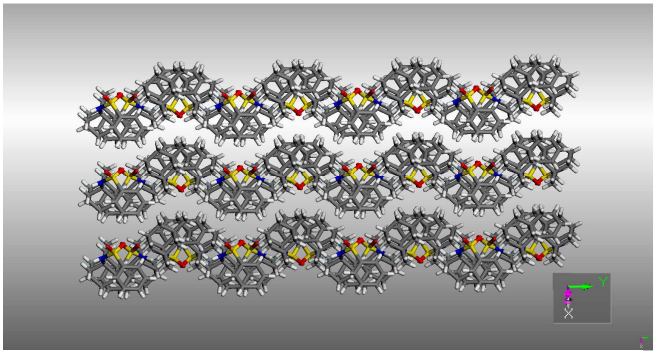

b

Fig. 9 Projections of molecular packing of crystal **5** on the planes (XOZ) – a and (201)– b

It is especially obvious in a projection on the plane (XOZ) (Fig. 9 a) containing a layered structure with alternately interlacing layers, composed by phenyl and adamantane molecular fragments. However, in contrast to the previous molecular packing, a subdivision of the adamantane motifs into pairs is

observed within the layer. This observation can probably be explained by the rotation of the adamantane fragment (see above), where the methyl groups are situated on the periphery of these pairs and promote such decoration of the layer. It is most probably this structurization that allows one of the molecular packing projections to be represented as a zigzag layer structure (Fig. 9 b).

Crystal structure data gives opportunity to calculate a free volume per molecule (V^{free}) in a crystal and analyze molecular packing by using $\beta = V^{free}/V^{vdw}$ parameter. This parameter shows how much the free volume increases as the molecular van der Waals's volume grows. The value of the discussed parameter depends on the molecular topology, the nature of atoms and the availability of hydrogen bond networks. The experimental value of β-parameter is a result of crystal lattice Gibbs energy minimization, including both enthalpic and entropic terms.

The dependence of the β-parameter on V^{vdw} is shown in Fig. 10.

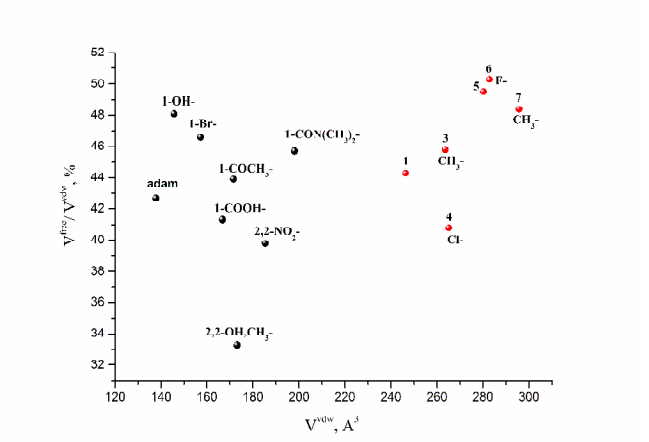

Fig. 10 Dependence β-parameter (V^{free}/V^{vdw}) versus V^{vdw} (adam – Adamantane; i-R- - i-R-Adamantane). Numbering correcponds to the compounds studied (red color points).

Beside the crystal structures studied in this work, we selected structures of adamantane and their derivatives from CSD,[34] the sublimation characteristics of which had been earlier described in literature. This step was aimed at finding out the regularities between the crystal structures of the substances and their sublimation thermodynamic functions (see below). Introducing substitutes COOH-, 2-di-NO_2 and 2,2-OH-, CH_3- into the adamantane molecule leads to denser molecular packing in the crystals (β-parameter decrease). In turn, introducing substitutes 1-OH-, 1-Br-, 1-$COCH_3$- and 1-$CON(CH_3)_2$- results in a decrease in the molecular packing density. It should be mentioned that both groups contain crystal structures with hydrogen bond networks. Therefore, the observed molecular packing changes are not connected with the factor.

Similar analysis can be done for compound **1** (as the initial one) and its derivatives - **3** and **4**. Introducing a Cl- atom at the para- position of the phenyl motif leads to an increase in the molecular packing density of the crystal, whereas introducing a methyl group at the same position produces the opposite effect. It should be mentioned, that compound **1** has no hydrogen bonds unlike the other two substances where infinite chains are observed.

If the crystal structures of adamantane and compound **1** are compared, introducing a phenyl sulfonamide fragment into 1-position does not practically lead to any changes in the molecular packing density. Adding two methyl groups to the adamantane fragment of molecule **1** (which results in the formation of compound (**5**)) leads to an essential reduction in the molecular packing density. Moreover, hydrogen bond networks are formed in the crystal structure. Introducing a methyl group at the para-position of the phenyl ring of molecule **5** (which results in the formation of compound (**7**)) leads to a decrease in the molecular packing density of the crystal, whereas adding an F- atom (compound **6**) has the opposite effect. The considered crystals also have hydrogen bond networks. Thus, the molecular packing densities of the crystals with adamantane motifs significantly depend on the molecular topology and substituents nature.

Sublimation Characteristics

The temperature dependences of saturated vapor pressure of **1, 2, 3, 4, 6, 7** are shown in Table 1ESI. The thermodynamic functions of sublimation and fusion processes of the selected substances are presented in Table 4.

Table 4. Thermodynamic characteristics of sublimation and fusion processes of the compounds studied

	1	**2**	**3**	**4**	**6**	**7**
ΔG^{298}_{sub} [kJ·mol^{-1}]	59.6	59.8	70.2	65.2	58.2	58.8
ΔH^{T}_{sub} [kJ·mol^{-1}]	119.1 ± 0.8	116.5 ± 1.2	148.1 ± 1.3	120.1 ± 1.4	115.4 ± 1.6	108.8 ± 1.8
ΔH^{298}_{sub} [kJ·mol^{-1}]	123.6 ± 0.8	121.4 ± 1.2	154.4 ± 1.3	126.2 ± 1.4	120.8 ±1.6	115.1 ± 1.8
$C^{298}_{p,cr}$ [J·mol^{-1}·K^{-1}][a]	373.2	389	400.8	392.9	451	462.8
$T \cdot \Delta S^{298}_{sub}$ [kJ·mol^{-1}]	64.0	61.6	84.2	61.0	62.2	56.3
ΔS^{298}_{sub} [J·mol^{-1}·K^{-1}]	215 ± 6	207 ± 6	282 ± 8	205 ± 6	209 ± 7	189 ± 7
ς_H [%][b]	65.9	66.3	64.7	67.4	66.0	67.2
ς_{TS} [%][b]	34.1	33.7	35.3	32.6	34.0	32.8
T_m [K]	397.4 ± 0.2	419.3 ± 0.2	437.8 ± 0.2	459.9 ± 0.2	410.4 ± 0.2	435.5 ± 0.2
ΔH^{T}_{fus} [kJ·mol^{-1}]	14.7 ± 0.5	18.8 ± 0.5	25.9 ± 0.5	25.3 ± 0.5	29.8 ± 0.5	29.6 ± 0.5
ΔS^{T}_{fus} [J·mol^{-1}·K^{-1}][c]	37.0	44.8	59.2	55.0	72.6	68.0

[a] $C_{p,cr}^{298}$ has been calculated by Chikcos additive scheme[27] the error of the calculation procedure corresponds to significant digit;

[b] $\varsigma_H = (\Delta H_{sub}^{298} / (\Delta H_{sub}^{298} + T \cdot \Delta S_{sub}^{298})) \cdot 100\%$; $\varsigma_{TS} = (T \cdot \Delta S_{sub}^{298} / (\Delta H_{sub}^{298} + T \cdot \Delta S_{sub}^{298})) \cdot 100\%$;

[c] $\Delta S_{fus}^{T} = \Delta H_{fus}^{T} / T_m$;

Unfortunately, the sublimation thermodynamic characteristics of the studied class of compounds are not directly connected to the characteristics of crystal lattice structure such as V_{mol}, V^{free} and β-parameter. Nevertheless, we tried to find a correlation of the obtained thermodynamic functions and van der Waals's molecular volumes (V^{vdw}). The choice of this parameter as a descriptor was determined by the following reasons. Firstly, this value can be easily calculated on the basis of the structural formula of a substance. Secondly, the dominant interactions between the molecules of the chosen class in the crystal lattice are the non-specific (van der Waals) interactions. Table 2ESI (supporting information) summarizes the literature data and references used about the sublimation thermodynamic characteristics and fusion processes of adamantine and its derivatives, which are used in this analysis. The experimental data of sublimation Gibbs energies (ΔG_{sub}^{298} - a) and enthalpies (ΔH_{sub}^{298} - b) versus V^{vdw} are presented in Fig. 11. It is evident that our assumptions have been confirmed because a correlation was observed between the discussed values. Moreover, Gibbs energies can be described by the following correlation equation with good correlation characteristics:

$$\Delta G_{sub}^{298} = (-13.2 \pm 5.1) + (0.259 \pm 0.024) \cdot V^{vdw} \quad (6)$$

R = 0.922; σ = 6.39; n=23

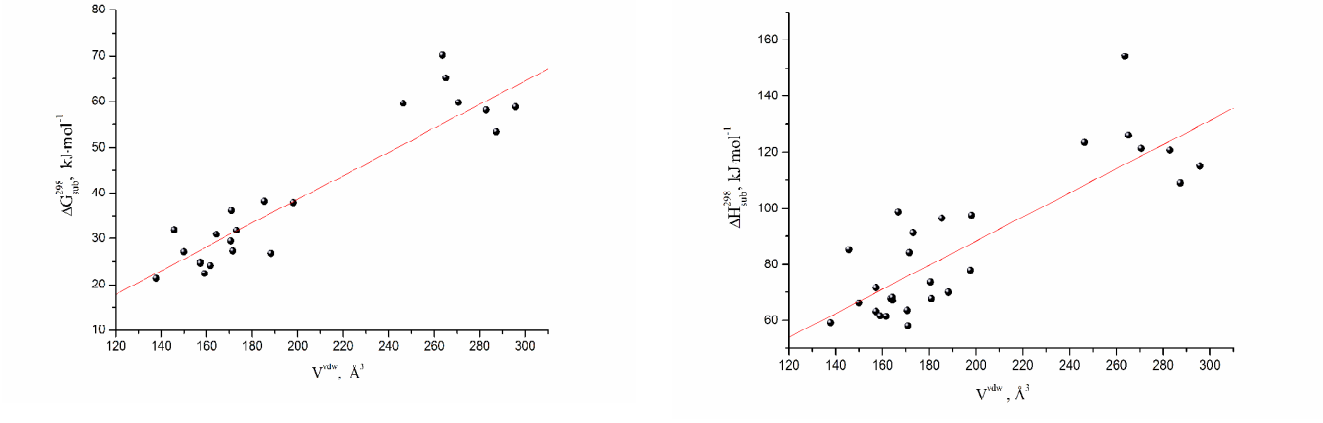

a b

Fig. 11 Dependencies of sublimation Gibbs energies (ΔG_{sub}^{298} - a) and enthalpies (ΔH_{sub}^{298} - b) versus V^{vdw}

Moreover, we tried to analyze the sublimation characteristics by HYBOT (**HY**drogen **BO**nd **T**hermodynamics) physicochemical descriptors.[30] The statistical analysis of the experimental data shows that the descriptors indicating polarizability (α/Å^3) of the molecule (a contribution made by non-specific interactions in the crystal lattice) and the sum of H-bond acceptor factors (ΣC_a) (a contribution made by specific interactions in the crystal lattice) are the best to describe the selected characteristics. The correlation equation can be presented as:

$$\Delta G_{sub}^{298} = (-8.8 \pm 3.5) + (1.69 \pm 0.17) \cdot \alpha + (4.2 \pm 1.4) \cdot \Sigma(C_a) \quad (7)$$

R=0.959; σ=4.81; F=113.8; n=23

$$\Delta H_{sub}^{298} = (14.0 \pm 7.2) + (2.71 \pm 0.33) \cdot \alpha + (6.3 \pm 1.9) \cdot \Sigma(C_a) \quad (8)$$

R=0.913; σ=10.8; F=67.9; n=30

Thus, all the sublimation thermodynamic functions of the compounds belonging to the selected class can be estimated based on the compound structural formula alone.

At the next stage of the investigation, we tried to estimate the contributions of various motifs of the studied molecules into the crystal lattice packing energy. In order to make the results of the calculations comparable to each other, we divided the selected molecule into three fragments for convenience (Scheme 3). The first one (I) includes the phenyl ring together with substitutes (if there are any). The second fragment (II) includes the sulfonamide bridge. Finally, the third fragment consists of the adamantane part with substituents.

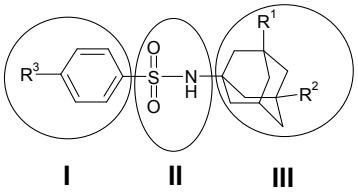

Scheme 3

The calculation results of the fragments contributions (with the hydrogen bonds energies taken into account) to the total packing energy versus β-parameter are presented in Fig. 12.

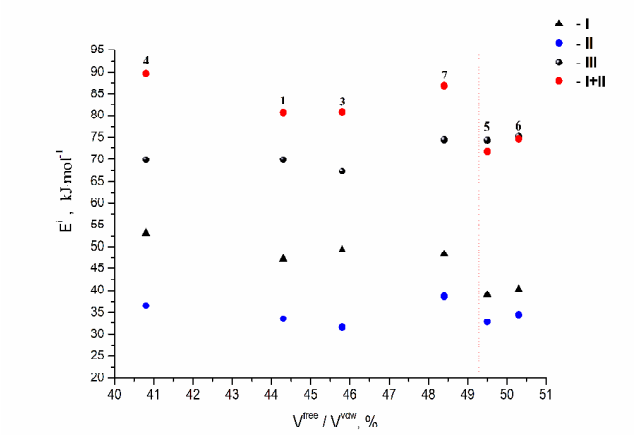

Fig. 12 Molecular fragments contributions (with the hydrogen bonds energies taken into account) to the total packing energy versus β-parameter (V^{free} / V^{vdw}). The red points correspond to the sum of the contribution made by fragments I and II

The red points correspond to the sum of the contribution made by fragments I and II. These energy contributions are comparable to the analogous contributions made by the big adamantane motif. Firstly, it should be noted that the discussed energetic terms can be ranged in the following way: E(II) < E(I) < E(III). Moreover, the energy term of the adamantane motif (for all the studied substances) is 1.5 times higher than that of the phenyl term (I). The sum of the first and second terms usually exceeds the analogous term of the adamantane motif (red points). When the crystal lattice molecular packing density reaches the critical value (in our case $\beta^* \approx 49.5$ %), the sum of the packing terms of fragments I and II, on the one side, and the packing term of the adamantine motif, on the other side, (**5**, **6**) are comparable. In other words, before the packing density reaches the critical value, the dominant contributions to the packing energy are made by the adamantane fragments. When the critical value is reached, the adamantine fragment competitors start making energy contributions to the packing energy.

In our previous works,[35] we found out a correlation between the melting points and free volumes per molecule in crystal lattices. The physical sense of such observation is connected to the fact that the free volume plays the role of crystal defects which, as a rule, determine fusion and sublimation processes.[36] For these regularities to be obtained the analyzed molecular structures should be similar and the crystal lattices of the compounds should have similar hydrogen bond networks. Taking into account this fact, we added 1-OH-Adamantane (RefCode Adamol)[34] to the studied compounds as the selected crystal structure has the same helicoids as crystals **3** and **4**. Compound **1** was excluded from consideration as there are no hydrogen bond networks in its crystals. Fig. 13 shows the dependence of the experimental melting points on the free volumes per molecule. As it follows from Fig. 13, an increase in the free volumes per molecule in the crystals results in the melting point values reduction.

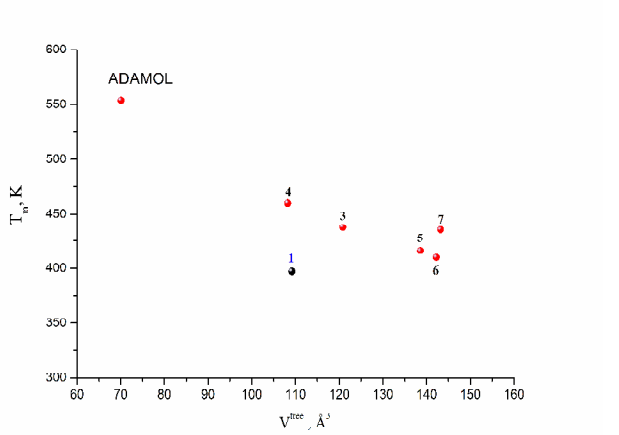

Fig. 13 Dependence of the experimental melting points versus the free volumes per molecule (V^{free}) in the crystal lattices studied

Conclusions

The crystal structures of six adamantane derivatives of sulfonamides have been solved by X-ray diffraction experiments. Comparative analysis of molecular conformational states has been carried out. It has been established that the mobility of the bridge connecting the phenyl and the adamantine fragments is very sensitive both to the free volume per a molecule in a crystal and to the presence of hydrogen bonds in which the bridge is involved. As the free volume per molecule in a crystal grows, the values τ_1, (τ_1 + τ_2) and ∠Ph-Ad decrease tending to the most unstrained state.

Parameter β has been introduced to describe the molecule packing density in crystals. Based on the X-ray results obtained in this study and those taken from other works, we analyzed the influence of the molecule topology and substituents nature on β-parameter for the crystals of this class. The molecular packing architecture of the selected crystals may be for convenience divided into three different groups.

The thermodynamic aspects of sublimation processes of the compounds were studied by determining the temperature dependence of vapor pressure using the transpiration method. A regression equation connecting the sublimation Gibbs energies and van der Waals's molecular volumes was derived. Moreover, correlations between the sublimation thermodynamic functions and physico-chemical descriptors such as ΣC_a (descriptor indicating the sum of H-bond acceptor factors – specific interactions) and polarizability of the molecule (non-specific interactions) were revealed.

The thermophysical characteristics of fusion processes of the molecular crystals were obtained and analyzed. A relationship between the melting points of the studied substances and the free volumes per molecule in the crystal lattices was evaluated. It was identified that an increase in the free volume per molecule in a crystal results in a decrease in the compounds melting points.

The influence of various molecular fragments on crystal lattice energy was analyzed. When the molecule packing density in a crystal reaches the critical value (in this case $\beta^* \approx 49.5$ %), the energy contributions to the packing energy made by the sum of fragments I (phenyl ring) and II (bridge), on the one side, and the adamantine fragment, on the other, are comparable. In other

words, before the packing density reaches the critical value, the dominant contributions are made by the adamantine fragments. When the critical value is reached, contributions are made by the adamantine fragment competitors determining the packing energy.

Acknowledgment

This work was supported by the Russian Scientific Foundation (№14-13-00640). We thank "the Upper Volga Region Centre of Physicochemical Research" for technical assistance with DSC experiments.

Notes and references

[a] *Krestov's Institute of Solution Chemistry, Russian Academy of Sciences, 153045 Ivanovo, Russia. Fax: +7 4932 336237; Tel: +7 4932 533784; E-mail: glp@isc-ras.ru*

[b] *Institute of Physiologically Active Compounds, Russian Academy of Sciences, 142432, Chernogolovka, Russia.*

[c] *Laboratory of Structural Chemistry, Institute of Problems of Chemical Physics, Russian Academy of Sciences, 142432, Chernogolovka, Russia*

† Electronic Supplementary Information (ESI) available: [The cif files of the 1, 3-7 compounds. Temperature dependences of saturation vapor pressure of the substances studied. Thermodynamic characteristics of sublimation and fusion processes of adamantane derivatives selected from literature. Geometry of the dimers of some compounds studied.]. See DOI: 10.1039/b000000x/

‡ Footnotes should appear here. These might include comments relevant to but not central to the matter under discussion, limited experimental and spectral data, and crystallographic data.

1 T. Owa, and T. Nagasu, *Exp. Opin. Ther. Patents,* 2000, **10**, 1725.
2. J. Drews, *Science,* 2000, **287**, 1960.
3. A.E. Boyd III, *Diabetes*, 1988, **37**, 847.
4. C.T. Supuran, and A. Scozzafava, *Expert. Opin. Ther. Pat.*, 2000, **10**, 575.
5. C.T. Supuran, and A. Scozzafava, *Curr. Med. Chem. Immunol. Endocr. Metab. Agents.*, 2001, **1**, 61.
6. R. Kasimogullari, M. Bulbul, H. Gunhan, and H. Guleryuz, *Bioorg. Med. Chem.*, 2009, **17**, 3295.
7. F. Abbate, A. Casini, T. Owa, A. Scozzafava, and C.T. Supuran, *Bioorg. Med. Chem. Lett.*, 2004, **14**, 217.
8. M.M.F. Ismail, M.M. Ghorab, E. Noaman, Y.A. Ammar, H.I. Heiba, and M.Y. Sayed, *Arzneim Forsch*, 2006, **56**, 301.
9. C.T. Supuran, and A. Scozzafava, *Expert. Opin. Ther. Pat.,* 2000, **10**, 575.
10. R.I. Olsson et al. *Bioorg. Med. Chem. Lett.*, 2014, **24**, 1269.
11. E. Rosatelli et al. *Bioorg. Med. Chem. Lett.*, 2014, **24**, 3422.
12. K. Gerzon, E.V. Krumalns, R.L. Brindle, F.J. Marshall, and M.A. Root, *J. Med. Chem.*, 1963, **6**, 760.
13. R.T. Rapala, R.J. Kraay, and K. Gerzon, *J. Med. Chem.*, 1965, **8**, 580.
14. K. Gerzon, and D. Kau, *J. Med. Chem.*, 1967, **10**, 189.
15. W.L. Davies, R.R. Grunert, R.F. Haff, J.W. McGahen, E.M. Neumayer, M. Paulshock, J.C. Watts, T.R. Wood, E.C. Hermann, and C.E. Hoffmann, *Science*, 1964, **144**, 862.
16. A. Tsunoda, H.F. Maassab, K.W. Cochran, W.C. Eveland, *Antimicrob. Agents Chemother.*, 1965, 553.
17. K.S. Rosenthal, M.S. Sokol, R.L. Ingram, R. Subramanian, and R.C. Fort, *Antimicrob. Agents Chemother.*, 1982, **22**, 1031.
18. Y. Dong, J. Chollet, H. Matile, S.A. Charman, F.C. Chiu, W.N. Charman, B. Scorneaux, H. Urwyler, J. Santo Tomas, C. Scheurer, C. Snyder, A. Dorn, X. Wang, J.M. Karle, Y. Tang, S. Wittlin, R. Brun, and J.L. Vennerstrom, *J. Med. Chem.*, 2005, **48**, 4953.
19. X. Wang, Y. Dong, S. Wittlin, D. Creek, J. Chollet, S.A. Charman, J. SantoTomas, C. Scheurer, C. Snyder, and J.L. Vennerstrom, *J. Med. Chem.*, 2007, **50**, 5840.
20. P.A. Swift, M.L. Stagnito, G.B. Mullen, G.C. Palmer, and V.S. Georgiev, *Eur. J. Med. Chem.*, 1988, **23**, 465.
21. R.S. Schwab, A.C. England Jr., D.C. Poskanzer, and R.R. Young, *J. Am. Med. Assoc.*, 1969, 208, 1168.
22. S.A. Lipton, *Nat. Rev. Drug Discovery*, 2006, **5**, 160.
23. *CAD-4 Software, Version 5.0; Enraf-Nonius: Delft*, The Netherlands, 1989.
24. G.M. Sheldrick, *SHELXL97 and SHELXS97*; University of Göttingen: Germany, 1997.
25. W. Zielenkiewicz, G. Perlovich, and M. Wszelaka-Rylik, *J. Therm. Anal. Calorim.,* 1999, **57**, 225.
26. J.D. Cox, and G. Pilcher, *Thermochemistry of Organic and Organometallic Compounds*, Academic Press: London,1970.
27. J.S. Chickos, and W.E. Acree Jr., *J. Phys. Chem. Ref. Data,* 2002, **31**, 537.
28. J.L. Pascual-Ahuir, E. Silla, *J. Comput. Chem.,* 1990, **11**, 1047.
29. A. Gavezzotti, and G. Filippini, Energetic aspects of crystal packing: Experiment and computer simulations. In *Theoretical Aspects and Computer Modeling of the Molecular Solid State*; Gavezzotti, A., Eds.; John Wiley & Sons: Chichester, 1997; Chapter 3, pp 61-97.
30. O.A. Raevsky, V.J. Grigor'ev, and S.V. Trepalin, HYBOT (Hydrogen Bond Thermodynamics) program package, *Registration by Russian State Patent Agency N 990090 of 26.02.99.*
31. M.C. Etter, *Acc. Chem. Res.,* 1990, **23**, 120.
32. J. Bernstein, R.E. Davis, L. Shimoni, and N-L. Chang, *Angew. Chem. Int. Ed. Engl.,* 1995, **34**, 1555.
33. G.L. Perlovich, A.M. Ryzhakov, V.V. Tkachev, L.Kr. Hansen, and O.A. Raevsky, *Cryst. Growth Des.*, 2013, **13**(9), 4002.
34. F.H. Allen, *Acta Crystallogr. B*. 2002, **B58**, 380.
35. A.M. Ryzhakov, Physicochemical properties of crystals and solutions of sulfonamides derivatives. PhD thesis. 2012. p. 160.
36. Yu.A. Lebedev, and E.A. Miroshnichenko, Thermochemistry vaporization of organic compounds. Heats of evaporation, sublimation and saturated vapor pressure. M: Nauka, 1981. p. 216.

Adamantane Derivatives of Sulfonamide Molecular Crystals: Structure, Sublimation Thermodynamic Characteristics, Molecular Packing, Hydrogen Bonds Networks

German L. Perlovich[*,†,‡], Alex M. Ryzhakov[†,‡], Valery V. Tkachev[‡,§], Alexey N. Proshin[‡]

[†]Krestov's Institute of Solution Chemistry, Russian Academy of Sciences, 153045 Ivanovo, Russia;
[‡]Institute of Physiologically Active Compounds, Russian Academy of Sciences, 142432, Chernogolovka, Russia;
[§]Laboratory of Structural Chemistry, Institute of Problems of Chemical Physics, Russian Academy of Sciences, 142432, Chernogolovka, Russia;

The crystal structures of six adamantane derivatives of sulfonamides have been determined by X-ray diffraction and their sublimation and fusion processes have been studied. Correlations between the sublimation thermodynamic functions and physico-chemical descriptors were revealed.

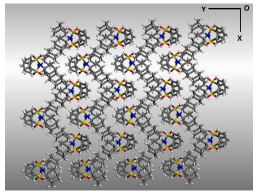

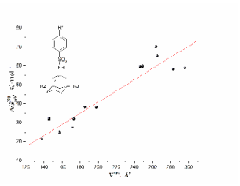

* To whom correspondence should be addressed:
Telephone: +7-4932-533784; Fax: +7-4932- 336237; E-mail glp@isc-ras.ru